# Electronic Supporting Information

# A comprehensive Brownian Dynamics approach for the determination of non-ideality parameters from analytical ultracentrifugation

*Maximilian J. Uttinger[1], Simon. E. Wawra[1], Tobias Guckeisen[1], Johannes Walter[1], Andreas Bear[3], Thaseem Thajudeen[2], Peter J. Sherwood[4], Ana Smith[3], Anja M. Wagemans[5], Walter F. Stafford[6] and Wolfgang Peukert[1*]*

AUTHORS ADDRESS

[1]Institute of Particle Technology, Interdisciplinary Center for Functional Particle Systems, Friedrich-Alexander-Universität Erlangen-Nürnberg, Haberstraße 9a, 91058 Erlangen, Germany

[2]School of Mechanical Sciences, Indian Institute of Technology, Goa College of Engineering Campus, Farmagudi, Ponda-403401,Goa, India

[3]PULS group, Department of Physics, Interdisciplinary Center of Nanostructured Films, Friedrich-Alexander-Universität Erlangen-Nürnberg (FAU), Cauerstrasse 3, 91058 Erlangen, Germany

[4]Interactive Technology Inc., P.O. Box 2768, Oakland, California 94602, USA

[5]Institute of Food Technology and Food Chemistry, Technical University Berlin, Königin Luise-Str. 22, 14195 Berlin, Germany

Department of Neurology, Harvard Medical School, 220 Longwood Avenue Goldenson Building, Boston, MA 02115USA

*[1]Corresponding Author: Wolfgang Peukert: +499131/85-29400, wolfgang.peukert@fau.de

**Brownian Dynamics Algorithm**

The position of each particle x is known at time t. In the case of concentration dependent sedimentation and diffusion coefficient, the displacement due to sedimentation, $\Delta x_{Sed}$, and diffusion, $\Delta x_{Brow}$, are given by:

$$x(t + \Delta t) = x(t) + \Delta x_{Sed} + \Delta x_{Brow} \quad (1)$$

$$\Delta x_{Sed} = x(t)[exp(s(c)\omega^2 \Delta t) - 1] \quad (2)$$

$$< \Delta x_{Brow}{}^2 >= 2D(c)\Delta t \quad (3)$$

The concentration dependence is implemented by correcting the sedimentation and diffusion coefficient to the local concentration $c_j$. This concentration is calculated based on the number of particles in each small compartment in the discretized cell, the so-called bins.

For the calculation of the local (bin) concentration, the volume of each individual subsection of the cell is considered (as indicated in the subsequent figure). Furthermore, the volume increase towards the bottom of the centrifugal cell ($V_{bin\#1} < V_{bin\#2}$) is taken into account within our algorithm. With this, we ensure that radial diluation effects are properly described.

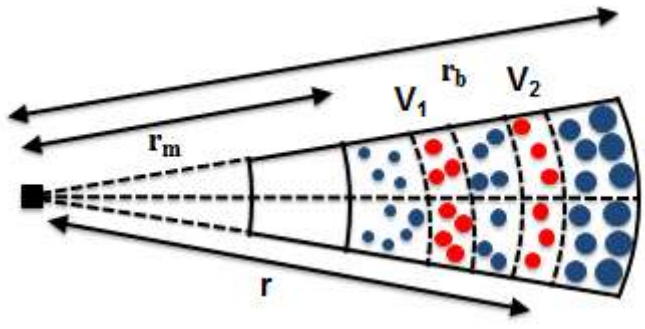


Figure S1: Schematic 2D representation of a sector-shaped AUC cell with meniscus positions $r_m$ and bottom position $r_b$. The cell is subdivided in several bins with width $\Delta r$ in order to calculate local concentrations and to produce output data. This representation is taken from literature and adapted for the purpose of the illustration.[1]

**Simulation of ideal sedimentation behavior**

For a thorough illustration, we performed SV AUC simulations via our BD algorithm for the lysozyme model system and the same experimental values as in the main manuscript considering ideal sedimentation behavior only. Obtained profiles for ideal sedimentation profiles are given in the subsequent figure.

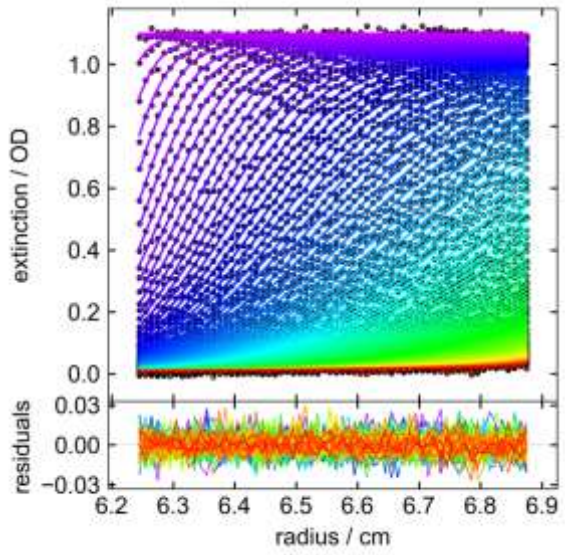


Figure S2: Left: Simulations from the BD algorithm (data points) and fit from numerical solutions of Lamm's Equation (straight lines) for ideal sedimentation behavior of the Lysozyme model system. The residual pattern shows no differences.

**Taylor Series Approximation up to third order**

As the movement of nanoparticles in a centrifugal field ought to be described, the displacement of a particle in a single time step is extended by a deterministic sedimentation displacement and thus considerably larger. Therefore, higher order terms will be considered for the local diffusion coefficient and the resulting displacement of the particles. This will enable to model larger displacements. The resulting expression is given as:

$$\Delta x_{Brow} = \pm\sqrt{2D[x(t)]\Delta t} + \alpha\frac{dD(c_j)}{dx}\Delta t \pm \frac{\alpha^2}{\sqrt{2}}\sqrt{D}\frac{d^2D(c_j)}{dx^2}\Delta t^{1.5} + \frac{\alpha^3}{3}D\frac{d^3D(c_j)}{dx^3}\Delta t^2 \quad (4)$$

**First Derivative**

$$\frac{\partial D}{\partial x} = \frac{\partial D}{\partial c}\cdot\frac{\partial c}{\partial x} \quad (5)$$

**Second Derivative**

$$\frac{\partial^2 D}{\partial x^2} = \frac{\partial}{\partial x}\left[\frac{\partial D}{\partial c}\cdot\frac{\partial c}{\partial x}\right] \quad (6)$$

$$\frac{\partial^2 D}{\partial x^2} = \left[\frac{\partial}{\partial x}\left(\frac{\partial D}{\partial c}\right)\right]\cdot\frac{\partial c}{\partial x} + \frac{\partial D}{\partial c}\cdot\left[\frac{\partial}{\partial x}\left(\frac{\partial c}{\partial x}\right)\right] \quad (7)$$

$$\frac{\partial^2 D}{\partial x^2} = \frac{\partial^2 D}{\partial c^2}\cdot\frac{\partial c}{\partial x}\cdot\frac{\partial c}{\partial x} + \frac{\partial D}{\partial c}\cdot\frac{\partial^2 c}{\partial x^2} \quad (8)$$

$$\frac{\partial^2 D}{\partial x^2} = \frac{\partial^2 D}{\partial c^2} \cdot \left(\frac{\partial c}{\partial x}\right)^2 + \frac{\partial D}{\partial c} \cdot \frac{\partial^2 c}{\partial x^2} \tag{9}$$

**Third Derivative**

$$\frac{\partial^2 D}{\partial x^2} = I + II \tag{10}$$

$$\frac{\partial^3 D}{\partial x^3} = \frac{\partial}{\partial x} I + \frac{\partial}{\partial x} II \tag{11}$$

$$\frac{\partial}{\partial x} I = \frac{\partial}{\partial x}\left[\frac{\partial^2 D}{\partial c^2} \cdot \left(\frac{\partial c}{\partial x}\right)^2\right] \tag{12}$$

$$\frac{\partial}{\partial x} I = \frac{\partial}{\partial x}\left[\frac{\partial^2 D}{\partial c^2} \cdot \left(\frac{\partial c}{\partial x}\right)^2\right] \tag{13}$$

$$\frac{\partial}{\partial x} I = \frac{\partial^3 D}{\partial c^3} \cdot \left(\frac{\partial c}{\partial x}\right)^3 + 2\frac{\partial^2 D}{\partial c^2} \cdot \frac{\partial c}{\partial x} \cdot \frac{\partial^2 c}{\partial x^2} \tag{14}$$

$$\frac{\partial}{\partial x} II = \frac{\partial}{\partial x}\left[\frac{\partial D}{\partial c} \cdot \frac{\partial^2 c}{\partial x^2}\right] \tag{15}$$

$$\frac{\partial}{\partial x} II = \frac{\partial^2 D}{\partial c^2} \cdot \frac{\partial c}{\partial x} \cdot \frac{\partial^2 c}{\partial x^2} + \frac{\partial D}{\partial c} \cdot \frac{\partial^3 c}{\partial x^3} \tag{16}$$

$$\frac{\partial^3 D}{\partial x^3} = \frac{\partial^3 D}{\partial c^3} \cdot \left(\frac{\partial c}{\partial x}\right)^3 + 2\frac{\partial^2 D}{\partial c^2} \cdot \frac{\partial c}{\partial x} \cdot \frac{\partial^2 c}{\partial x^2} + \frac{\partial^2 D}{\partial c^2} \cdot \frac{\partial c}{\partial x} \cdot \frac{\partial^2 c}{\partial x^2} + \frac{\partial D}{\partial c} \cdot \frac{\partial^3 c}{\partial x^3} \quad (17)$$

**Derivation of Diffusion coefficient over concentration**

$$\frac{dD(c_j)}{dc_j} = D_0 \frac{\beta - k_s}{(1 + k_s c_j)^2}) \quad (18)$$

$$\frac{d^2 D(c_j)}{dc_j{}^2} = D_0 \frac{2(\beta - k_s)k_s}{(1 + k_s c_j)^3}) \quad (19)$$

$$\frac{d^3 D(c_j)}{dc_j{}^3} = D_0 \frac{6(\beta - k_s)k_s^2}{(1 + k_s c_j)^4} \quad (20)$$

## Iterative test of Equation 12 in main manuscript

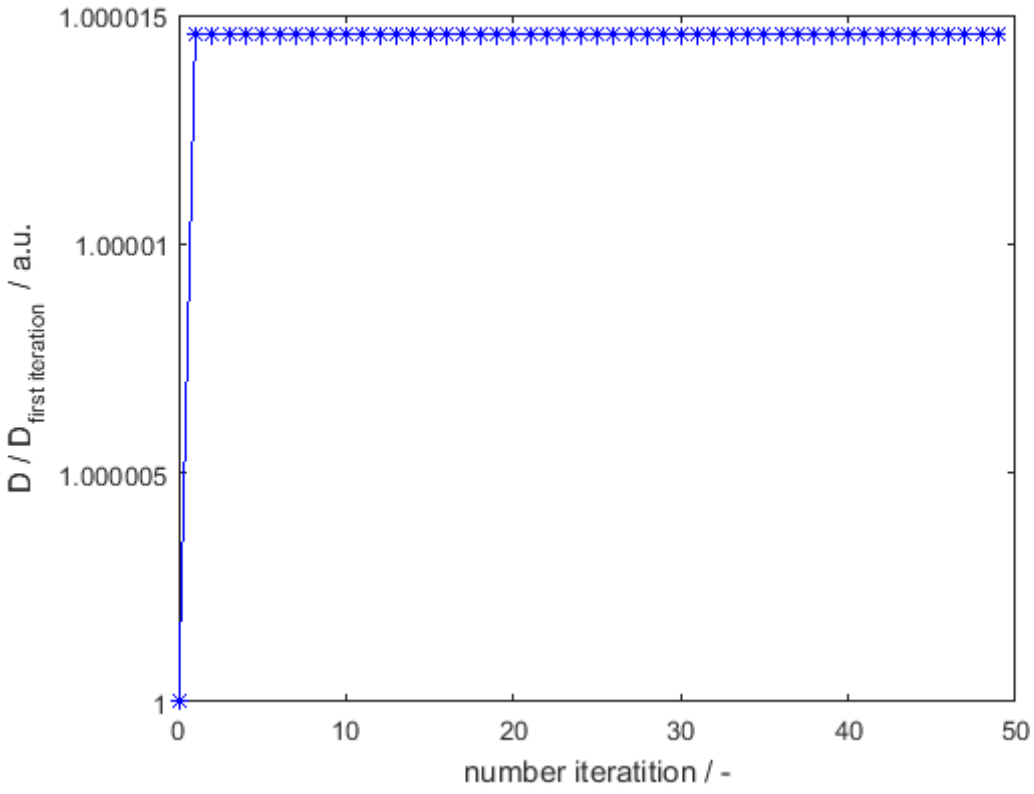


Figure S3: Diffusion coefficient as input to Equation 12 in the main manuscript. The diffusion coefficient is calculated from numerous iterations as depicted in Figure 1 of the main manuscript.

**Underlying theory of the evaluation tool SEDANAL**

At the meniscus and cell base, the sedimentation and diffusion fluxes are equal to zero. Therefore no solute can cross the meniscus or base of the cell, hence defining the boundary conditions of the numerical solution. In the case of ideal sedimentation and no interactions, such as chemical reactions, between concurrently sedimenting species, there is a separate Partial Differential Equation (PDE) for each species. Thus, the finite-element method (FEM) formulation to Lamm's Equation for the ideal case is given by Todd and Haschemeyer[2]:

$$Gc_{+} = Z \; and \; Z = Hc_{-}$$
$$with \; G = \left(B + \Delta t(D_0 A^1 - s_0 \omega^2 A^2)\right) \tag{21}$$

A1 and A2 are tridiagonal matrices which are only dependent upon the grid chosen for the FEM. The components of the vector c are concentrations at each grid point (+ and – refer the start and end of each time step). Non-ideality is introduced as hydrodynamic and thermodynamic, with the coefficients BM and $k_s$. The diffusion and sedimentation coefficients are functions of concentration, so at each radial grid point:

$$s = s_0(1-\theta) and \; D = D_0(1-\varepsilon)$$
$$with \; \varepsilon = \frac{Q-P}{1+Q} and \; \theta = Q/(1+Q) \tag{22}$$
$$with \; P = (2BM \cdot c) and \; Q = k_s \cdot c$$

Once ε and Θ are known for each radial grid point, the vectors $C^U$, $C^V$, $C^W$ and $C^A$ are computed as:

$$c_i^U = c_{i+1} + 1\theta_i$$
$$and \; c_i^V = c_i\theta_i \tag{23}$$

$$and\ c_i^W = c_i\theta_{i+1}$$

$$and\ c_i^{\mathrm{A}} = c_i\varepsilon_i$$

The correction for non-ideality, y, is given by:

$$y = \Delta t(D_0(UC^U + VC^V + WC^W) - s_0\omega^2A^2C^A \quad (24)$$

U, V, and W are tridiagonal matrices dependent only on the grid. The correction for non-ideality is added to Z, so:

$$Z = Bc_- + y \quad (25)$$

In case of chemical reactions, SEDANAL perform alternating steps in the of sedimentation/diffusion and chemical kinetics/equilibria. The algorithm analyses SE data by fitting sedimentation data to an equation of the form:

$$y - y_0 = \sum_{i=1}^{n_s} A_i \exp(kM_i\xi + 2\sum_{j=1}^{n_s} B_jc_j \quad (26)$$

$$with\ A_i = c_i(r_m)\gamma_i\ and\ \xi = \frac{r^2}{2} - \frac{r_m^2}{2} \quad (27)$$

Here, y is the signal and $y_0$ an offset. The term $\mathbf{2}\sum_{\boldsymbol{j=1}}^{\boldsymbol{n_s}}\boldsymbol{B_jc_j}$ in the exponential contains the Non-Ideality of species *j*. The extinction coefficient of species *i* is denoted $\gamma_i$.

**Brownian Dynamics Simulations - Ideal Sedimentation behavior**

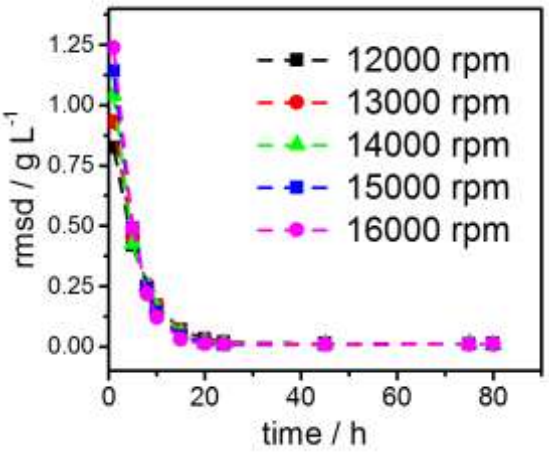


Figure S4: Time for equilibrium. The rmsd is calculated based on the difference of each scan and the first scan

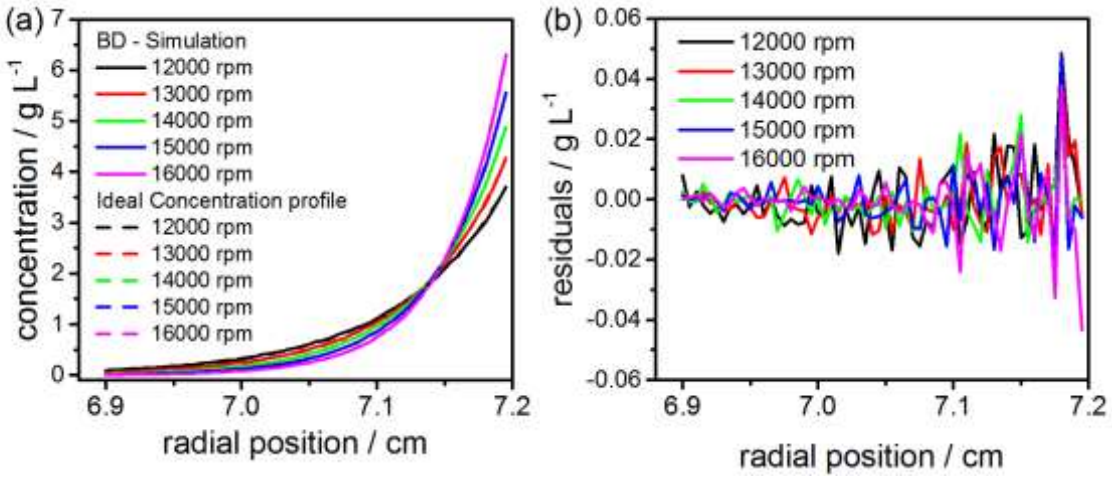


Figure S5 (a) Simulated SE profiles from BD simulation (straight lines) and the theoretically calculated ideal SE profiles (dashed lines) (b) Residuals of the profiles in (a) between the simulated and the theoretically calculated profiles.

Table S1: Parameters for ideal SE BD simulations. Values of further BD simulations with more species present are shown alongside the retrieved molar masses from SEDANAL.

| # | Rotor velocity/ rpm | $M_{in,BD}$ kDa | $M_{out,SA}$ kDa | Deviation % |
|---|---|---|---|---|
| 1 | 12000 | | 100.44 | 0.44 |
| 2 | 13000 | | 100.833 | 0.83 |
| 3 | 14000 | 100 | 100.44 | 0.44 |
| 4 | 15000 | | 100.71 | 0.71 |
| 5 | 16000 | | 100.84 | 0.84 |
| 6 | 7600 - 22000 | 50/100 | 51.87/103.67 | 3.37/3.57 |
| 7 | 6200 - 20000 | 100/150 | 102.70/167.54 | 2.70/11.69 |
| 8 | 6200 - 22000 | 50/150 | 50.73/154.71 | 1.45/3.14 |

**Derivation of non-ideal sedimentation equilibrium**

$$\overrightarrow{J_D} = (-(1-\alpha)c\frac{dD}{dr} - D\frac{dc}{dr})\overrightarrow{e_r} \tag{28}$$

$$\overrightarrow{J_S} = csw^2r \cdot \overrightarrow{e_r} \tag{29}$$

$$D = D_0(\tfrac{1+\beta c}{1+k_s c}) \text{ mit } \beta = 2BM - \bar{v} \tag{30}$$

$$\frac{dD}{dr} = \frac{dD}{dc}\frac{dc}{dr} = D_0 c\left(\frac{\beta(1+k_s c) - (1+\beta c)k_s}{(1+k_s c)^2}\right)\frac{dc}{dr} \tag{31}$$

$$\overrightarrow{J_D} + \overrightarrow{J_s} = 0 \tag{32}$$

$$\begin{aligned}(1-\alpha)D_0 c\left(\frac{\beta(1+k_s c) - (1+\beta c)k_s}{(1+k_s c)^2}\right)\frac{dc}{dr} + D_0\left(\frac{1+\beta c}{1+k_s c}\right)\frac{dc}{dr} = \\ = \frac{s_0 c}{1+k_s c}\omega^2 r\end{aligned} \tag{33}$$

$$(1-\alpha)D_0\left(\frac{\beta(1+k_s c) - (1+\beta c)k_s}{1+k_s c}\right)\frac{dc}{dr} + D_0\left(\frac{1+\beta c}{c}\right)\frac{dc}{dr} = s_0\omega^2 r \tag{34}$$

$$\left[(1-\alpha)\left(\beta - \frac{k_s + \beta k_s c}{1+k_s c}\right) + \frac{1}{c} + \beta\right]dc = \frac{s_0}{D_0}\omega^2 r dr \tag{35}$$

$$\frac{k_s+\beta k_s c}{1+k_s c}=\frac{k_s}{1+k_s c}+\frac{\beta k_s c+\beta-\beta}{1+k_s c}=\frac{k_s}{1+k_s c}+\frac{\beta(1+k_s c)}{1+k_s c}-\frac{\beta}{1+k_s c}$$
$$=\frac{k_s-\beta}{1+k_s c}+\beta \tag{36}$$

$$\int \frac{k_s-\beta}{1+k_s c}dc=\frac{(k_s-\beta)}{k_s}\cdot \ln(1+k_s c)+C \tag{37}$$

$$\left[(1-\alpha)\left(-\frac{k_s-\beta}{1+k_s c}\right)+\frac{1}{c}+\beta\right]dc=\frac{s_0}{D_0}\omega^2 r dr \tag{38}$$

$$\int_{c_0}^{c}\ldots=\int_{r_0}^{r}\ldots \tag{39}$$

$$-(1-\alpha)\frac{k_s-\beta}{k_s}ln\left(\frac{1+k_s c(r)}{1+k_s c(r_0)}\right)+ln\left(\frac{c(r)}{c(r_0)}\right)+\beta\big(c(r)-c(r_0)\big)$$
$$=\frac{1}{2}\frac{s_0}{D_0}\omega^2(r^2-r_0^2) \tag{40}$$

**Accordance of NI SE BD simulations and the analytical solution of equation 7 of the main manuscript**

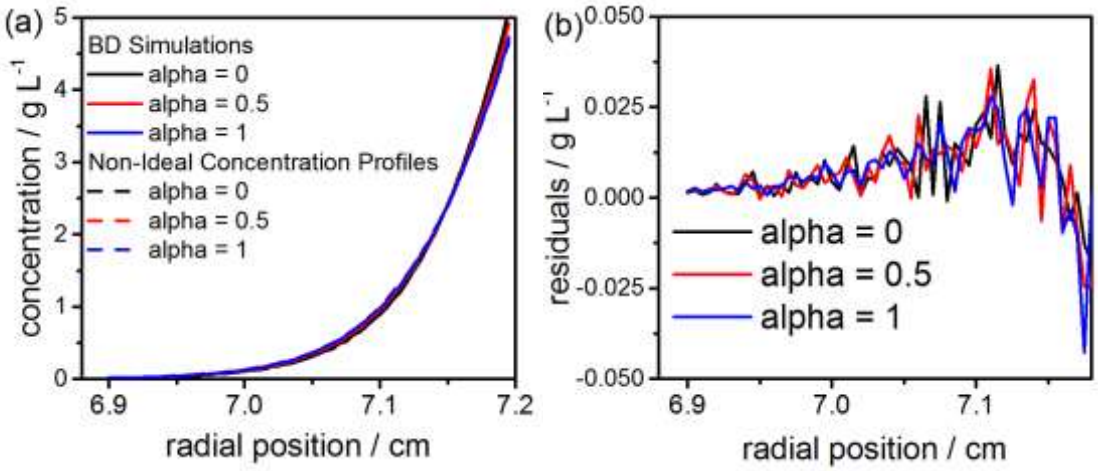


Figure S6(a) Simulated SE profiles by the BD algorithm for different values of α for a model system with a molar mass of 100 kDa and the non-ideality parameters $k_s$ = 250 mL $g^{-1}$ and BM = 75 mL $g^{-1}$ (straight lines) and numerically calculated profiles (dashed lines) The rotor speed was set to 12000 rpm. (b) Residuals of the profiles in (a).

## Inclusion and exclusion of hydrodynamic non-ideality throughout BD simulations

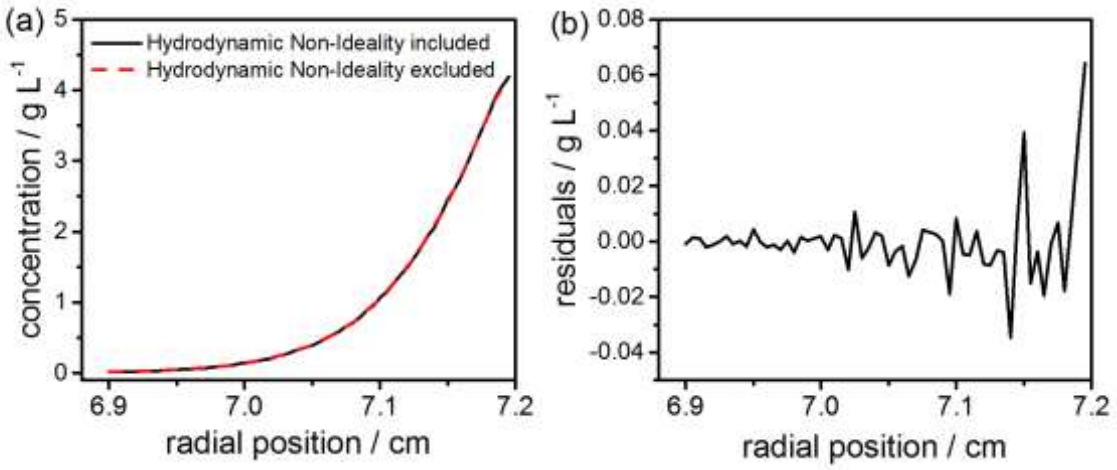


Figure S7:(left) Simulated SE profiles with no hydrodynamic non-ideality (dashed line, ks = 0 mL g-1) and including hydrodynamic non-ideality (straight line, ks = 100 mL g-1) for a theoretical model system with a molar mass M = 100 kDa at a rotor speed of 12000 rpm. (right) Residuals of the profiles in (a).

**Results from BD simulation describing the space-dependent diffusion coefficient with a Taylor Series Approximation up to third order**

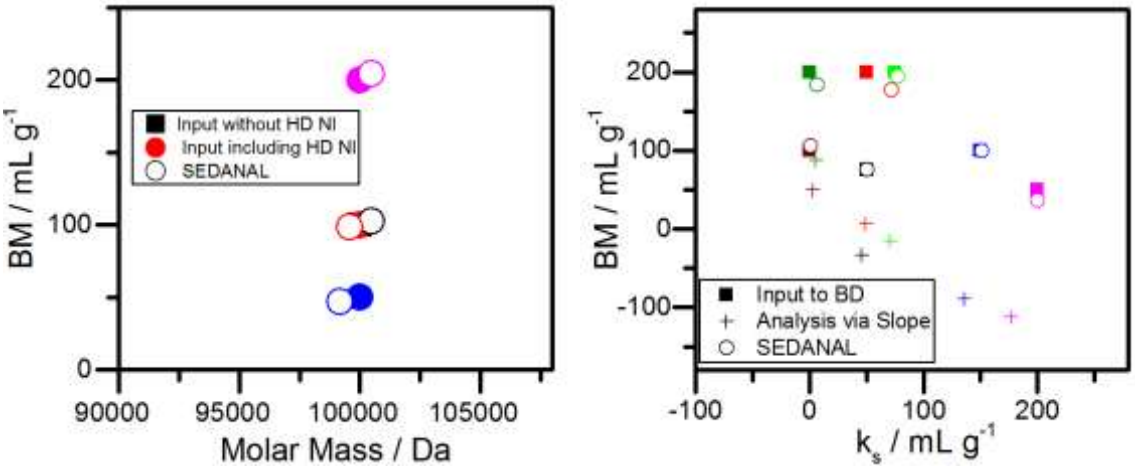


Figure S8(Left)**:** Retrieved values from data analysis of SE BD forward simulations in SEDANAL along the input values to the BD simulations. (Right):Retrieved values from data analysis of SV BD forward simulations in SEDANAL (open circles) along the input values to the BD simulations (square symbols). The results from the slope-analysis are presents as cross-symbols.

## Analysis of the slope from BD simulations

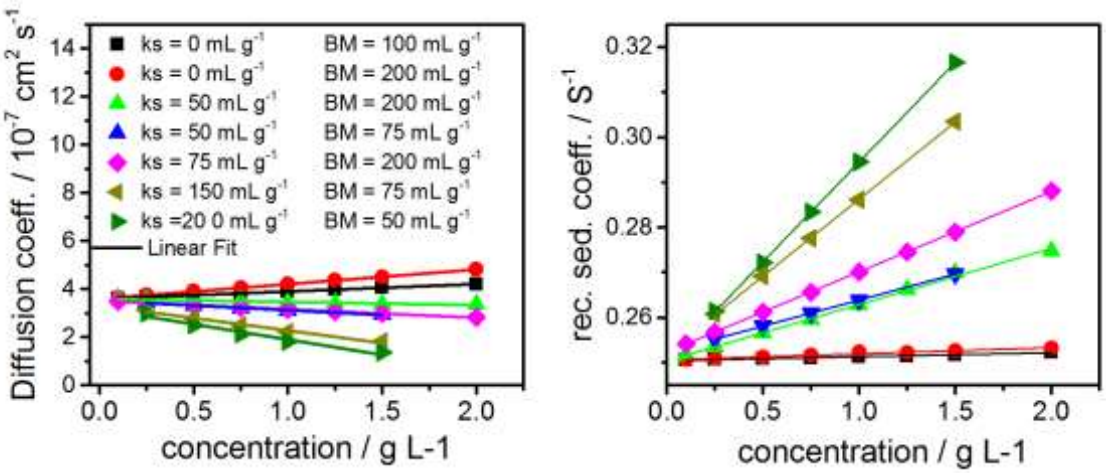


Figure S9: (Right) Apparent reciprocal Sedimentation coefficient versus loading concentration. (Left). Apparent diffusion coefficient is shown as a function of the loading concentration. Data are shown along with the theoretically calculated values for the known parameters. Values were extracted from the ideal single species model of SEDFIT.

## Analysis of the slope from experimental data

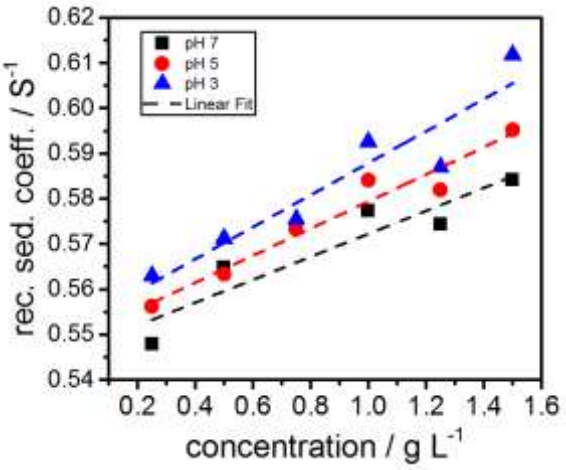


Figure **S**10: Apparent reciprocal sedimentation coefficient as a function of the loading concentration for the model system lysozyme. The slope gives $k_s$.

## Experimental Data for Membrane Osmometry

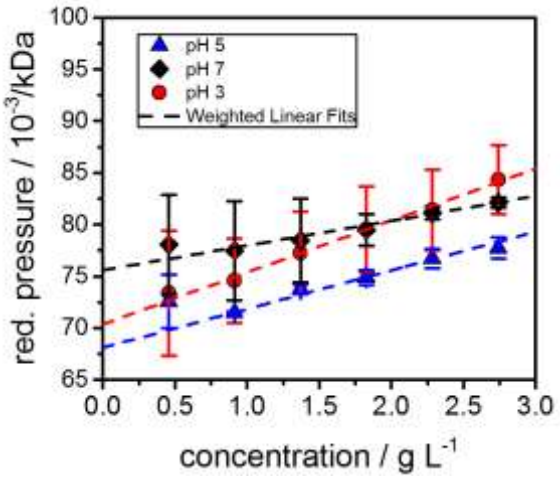


Figure S11: Results from membrane Osmometry measurements different lysozyme concentrations. Linear fits yield the second virial coefficient alongside the molar mass at infinite dilution.

**Correlation of non-ideality parameters from SV-AUC experiments and DLVO theory**

In the context of the DLVO theory, the interaction potential φ(x) is calculated from considering three contributions, namely an electrostatic potential, a Van-der-Waals (VDW) potential and an osmotic potential.[3] Details of the calculation are presented in the ESI.

$$\varphi(r) = \varphi_{osm}(r) + \varphi_{el}(r) + \varphi_{VDW}(r) \tag{41}$$

The osmotic potential is a function of the minimal distance between two protein molecules, which can be approximated by:

$$x_{23} = \frac{x_P + x_s + l_0}{2} \tag{42}$$

Here $x_P$ is the protein diameter, $x_S$ the diameter of the salt and $l_o$ the minimal distance, which is derived based on the data of van Oss $l_o$ as 0.1568 nm[4]. The salt diameter for sodium chloride is equal to 0.18 nm. The protein diameter is taken to be the hydrodynamic diameter. Consequently, the potentials can be expressed as:[5]

$$\varphi_{osm}(r) = -\frac{4}{3}\pi r_{23}^3 \rho_{s,N} k_B T \left(1 - \frac{3x}{4x_{23}} + \frac{x}{16x_{23}^3}\right) \tag{43}$$

$$\varphi_{el}(r) = \frac{Z^2 e^2 \exp((x_P - x))}{4\pi\varepsilon_0\varepsilon_r x(1 + \kappa x_P/2)^2} \tag{44}$$

$$\varphi_{VDW}(r) = -\frac{A_H}{12}\left[\frac{x_P^2}{x^2 - x_P^2} + \frac{x_P^2}{x^2} + 2\ln(1 - \frac{x_P^2}{x^2})\right] \tag{45}$$

The Debye length κ, which is a function of the ionic strength, is calculated from the well-known debye-Hückel theory.[6] The number density of the salt ions is denoted as $\rho_{S,N}$. Z is the number of charges on a protein molecule. For the calculations in the framework of this

manuscript, the values for Z were adapted from literature, based on the data from Haynes.[7] The Hamaker constant $A_H$ for lysozyme was taken from literature as $3.3x10^{-20}$ J.[8] For the purpose of this manuscript, the interaction potentials for lysozyme in a 10 mM NaCl solution were calculated at different pH values and corresponding number of charges for a lysozyme molecule. The potentials as a function of the separation distance are shown in the main manuscript.

**Simulated profiles for the interplay of hydrodynamic / thermodynamic non-ideality with solvent compressibility**

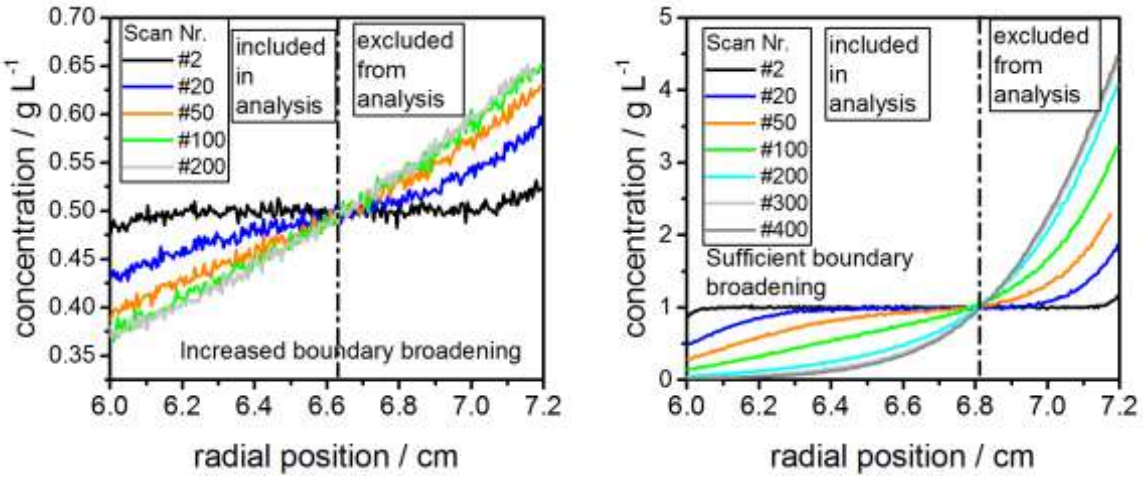


Figure S12: All parameters are given in the main manuscript. Profiles from BD simulations for model particles in toluene including solvent compressibility and concentration-dependent non-ideality are shown. Left: simulated profiles at 20,000 rpm. Right: Simulated profiles at 60,000 rpm.

# References

(1) Uttinger, M. J.; Walter, J.; Thajudeen, T.; Wawra, S. E.; Peukert, W. Brownian dynamics simulations of analytical ultracentrifugation experiments exhibiting hydrodynamic and thermodynamic non-ideality. *Nanoscale* **2017**, *2*, 200.

(2) Todd, G. P.; Haschemeyer, R. H. General solution to the inverse problem of the differential equation of the ultracentrifuge. *Proc. Natl. Acad. Sci. USA* **1981**, *78*, 6739–6743.

(3) Derjaguin, B.; Landau, L. Theory of the stability of strongly charged lyophobic sols and of the adhesion of strongly charged particles in solutions of electrolytes. *Prog. Surf. Sci.* **1993**, *43*, 30–59.

(4) van Oss, C. J. *Interfacial forces in aqueous media*, Second edition; Taylor & Francis: Boca Raton, Fla, 2006.

(5) Striolo, A.; Ward, J.; Prausnitz, J. M.; Parak, W. J.; Zanchet, D.; Gerion, D.; Milliron, D.; Alivisatos, A. P. Molecular Weight, Osmotic Second Virial Coefficient, and Extinction Coefficient of Colloidal CdSe Nanocrystals. *J. Phys. Chem. B* **2002**, *106*, 5500–5505.

(6) Curtis, R. A.; Prausnitz, J. M.; Blanch, H. W. Protein-protein and protein-salt interactions in aqueous protein solutions containing concentrated electrolytes. *Biotechnol. Bioeng.* **1998**, *57*, 11–21.

(7) Haynes, C. A.; Sliwinsky, E.; Norde, W. Structural and Electrostatic Properties of Globular Proteins at a Polystyrene-Water Interface. *J. Colloid Interface Sci.* **1994**, *164*, 394–409.

(8) Muschol, M.; Rosenberger, F. Interactions in undersaturated and supersaturated lysozyme solutions: Static and dynamic light scattering results. *J. Biol. Chem.* **1995**, *103*, 10424–10432.